MATHEMATICAL BIOSCIENCES
AND ENGINEERING
Volume **4**, Number **3**, July **2007**

http://www.mbejournal.org/

pp. **523–530**

PINNING CONTROL OF SPATIOTEMPORAL CHAOS IN THE LCLV DEVICE

Carolina Mendoza

Institute of Physics, Pontifical Catholic University of Valparaíso
234-0025 Valparaíso, Chile

Jean Bragard

Departamento de Física y Mat. Aplicada, Universidad de Navarra
31080 Pamplona, Spain

Pier Luigi Ramazza

CNR: Istituto dei Sistemi Complessi
Via Madonna del Piano 10, 50019 Sesto Fiorentino (FI), Italy

Javier Martínez–Mardones

Institute of Physics, Pontifical Catholic University of Valparaíso
234-0025 Valparaíso, Chile

Stefano Boccaletti

CNR: Istituto dei Sistemi Complessi
Via Madonna del Piano 10, 50019 Sesto Fiorentino (FI), Italy
Also at The Italian Embassy in Tel Aviv, Trade Tower
25 Hamered Street, Tel Aviv, Israel

(Communicated by Ying-Cheng Lai)

Abstract. We study the feasibility of transferring data in an optical device by using a limited number of parallel channels. By applying a spatially localized correcting term to the evolution of a liquid crystal light valve in its spatio–temporal chaotic regime, we are able to restore the dynamics to a specified target pattern. The system is controlled in a finite time. The number and position of pinning points needed to attain control is also investigated.

1. **Introduction.** An efficient data transfer by using all–optical systems in the chaotic regime is presently considered as an alternative to enhance the capability of information carriers [1]. A classical way to increase the capacity of optical networks is to use a technique called wavelength division multiplexing (WDM). The idea is to transmit data simultaneously at multiple carrier frequencies over an optical fiber [2]. An alternative to this technique is to use chaotic signals that are known to contain all the frequencies embedded inside the signals. In the past, a chaotic laser has already proven to be an useful tool for encoding and decoding information with high–speed data transfer [3, 4]. The communication systems are implemented using fiber optics. Another way of reaching high speeds of data transfer is using several

2000 *Mathematics Subject Classification.* 37D45.
Key words and phrases. chaos, LCLV system.

channels of information through parallel channels; and using a pinning technique to send target pattern [5].

In a recent letter, Pastur et al. [6] demonstrated experimentally that a state of spatiotemporal chaos in an optical device can be controlled by some appropriate optical perturbations introduced in the feedback loop. The present article is the theoretical counterpart of that letter. Here we address the following question: Is incomplete information sent to the system sufficient to stabilize a given target pattern? This matter is of practical importance, and it is related to the inherent losses that are always present in the transfer of signals through the fiber–optic network. Related topics have found a large echo in the scientific literature of this last decade and are gathered through the vocable of control and synchronization of chaotic systems [7, 8]. Several studies in the past have addressed the question of finding the minimal number of controllers needed to stabilize a desired state out of a spatiotemporal chaotic evolution [9, 10, 11] but in the context of the one dimensional complex Ginzburg-Landau equation. This equation, indeed, offers a universal description of any spatially extended system in the vicinity of a Hopf bifurcation [12]. Here, we specify this question for a given optical system, the liquid crystal light valve (LCLV), that has been widely used both experimentally and theoretically for describing chaotically evolving two–dimensional optical patterns.

The LCLV system has been extensively studied as an experimental model of optical device, because of its rather easy manipulation in physics laboratories and its large use in display media [13]. The main reason for this is the slow time scale that governs the pattern formation inside the LCLV, which is of order of one second. The pioneering works of lasers shining onto a Kerr media by Oppo et al. [14] have been followed by many experimental works on the LCLV [15, 16], which have revealed the richness of pattern formation in such nonlinear optical devices.

The experimental setup on which this theoretical work is based is described in full detail in reference [6] and will not be reported here. Using the standard eikonal approximation of wave optics [17], the equation that describes the evolution of the LCLV is [16]:

$$\frac{\partial \phi}{\partial t} = -\frac{\phi - \phi_0}{\tau} + D\nabla_\perp^2 \phi + \phi_{sat}(1 - e^{-\frac{\alpha I_0 I}{\phi_{sat}}}), \tag{1}$$

where the light intensity I is given by:

$$I = \mid BEe^{i\sigma\nabla_\perp^2} + C \mid^2, \tag{2}$$

and the electric field (E) and other parameters are:

$$E = e^{i\phi} \tag{3}$$

$$B = \cos(\theta_1)\cos(\theta_2) \tag{4}$$

$$C = \sin(\theta_1)\sin(\theta_2). \tag{5}$$

Here $\phi(x, y)$ is the phase of the optical beam at the output of the LCLV, ϕ_0 is the uniform phase obtained by opening the feedback loop, τ is the relaxation time of the liquid crystals inside the valve, ϕ_{sat} the value of phase saturation, α is a control parameter of the LCLV, I_0 is the intensity of the impinging laser beam, E the electric field, θ_1 is the angle between the input light and the LC director and θ_2 is the angle between the additional polarizer and the liquid crystal director. The beam is transmitted following the axis of the liquid crystal director, D is the diffusion constant of the phase inside the LCLV and L is the diffractive propagation length. Equation (1) is of the reaction-diffusion type and is also very common in

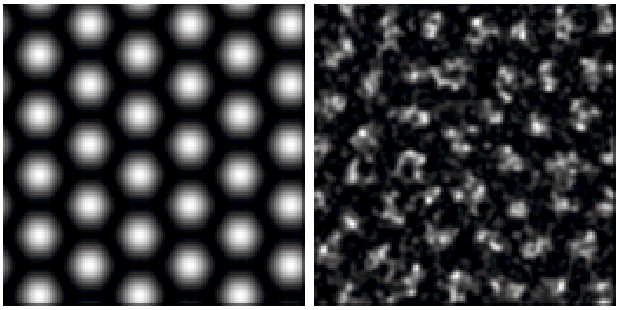

FIGURE 1. Snapshots of $\phi(x, y)$ obtained by integrating Eq.(1) with parameter value $\alpha I_0 = 0.6$ (left panel, stationary hexagons), and $\alpha I_0 = 1.7$ (right panel, spatiotemporal chaotic pattern).

the description of extended chemical reactors [18]. It is well known that these equations, under some general conditions, exhibit an instability leading to Turing patterns [19]. Therefore it is not surprising that simulation of Equation (1) leads to a stationary hexagonal pattern for small control parameter $\alpha I_0 = 0.6$ and to spatio-temporal chaos for larger value of the control parameter $\alpha I_0 = 1.7$, as shown in Figure 1.

2. **Control of spatiotemporal chaos.** The present work is based on numerical simulations of Equation (1). We have used a spectral method with 128x128 Fourier modes in the two spatial directions [20]. The time integration follows a Runge-Kutta scheme of the fourth order with a time step of ($\Delta t = 0.25$). The parameters used in the simulations which are relevant for comparison with the experimental setup are: $\theta_1 = \theta_2 = 0$, $D = 1.51\,10^{-8}\text{mm}^2/\text{s}$, $\phi_{sat} = 5\pi$ rad, $\sigma = 1\text{mm}^{-2}$, $\tau = 1\text{s}$, $\phi_0 = 0$, and $L_x = L_y = 2\text{mm}$. The wavelength of the laser light used in the experiment is $\lambda_0 = 633\text{nm}$.

The objective of this work is to test the feasibility of the control of spatio-temporal patterns in the LCLV. In particular, the number of points (in terms of the actual numerical grid) needed to control the pattern will be reduced as much as possible. As we are interested in future experimental implementation of this scheme, the perturbation term is written as a function of the light intensity rather than the phase of the electric field:

$$I_{pert} \quad = \quad I + c(I_t - I) \tag{6}$$

where c is the control strength and $I_t(x, y)$ is the intensity of the target pattern. The control is realized by replacing the intensity I by I_{pert} in Equation (1) at (and only at) the given locations of the selected pinning points.

Two different kind of localizations for the pinning points (the points where the control perturbation is applied) are used: regular and random. For the regular grid, $np = 1$ means that all grid points are pinning points, $np = 2$ corresponds to the situation of leaving a space between the pinning points in each directions, for $np = 3$ two mesh points are left uncontrolled in each directions between pinning points, and so on for larger values of np. Table 1 and Figure 2 summarize the number and location of the pinning points for different values of np in the regular

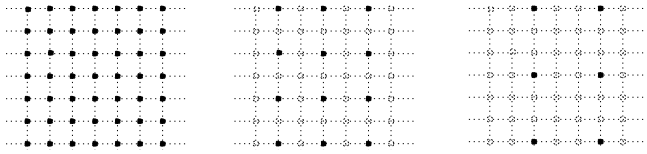

FIGURE 2. Schematic of the numerical grid. Black circles represent pinning points where the control is applied while open circles are not perturbed and follow Eq.(1). From left to right:$np = 1$; $np = 2$; $np = 3$.

case. For the random case, the number of points are the same as for the regular case but are distributed randomly over the numerical grid.

np	pinning points	pp	$\%pp$
1	128x128	16384	100
2	64x64	4096	25
3	43x43	1849	11.3
4	32x32	1024	6.25
5	26x26	676	4.13
6	21x21	441	2.69
7	18x18	324	1.98
8	16x16	256	1.56
9	14x14	196	1.20
10	13x13	169	1.03

TABLE 1. The first column refers to the parameter np, second and third columns refer to the total number of pinning points (pp), and the fourth column ($\%pp$) is the percentage of the pinning point with respect to the total number of grid points.

To quantify the ability of controlling the system, one defines the cross-correlation between the actual pattern and the desired target pattern as follows:

$$\rho = \frac{\langle (I - \langle I \rangle)(I_t - \langle I_t \rangle) \rangle}{\sqrt{\langle (I - \langle I \rangle)^2 \rangle} \sqrt{\langle (I_t - \langle I_t \rangle)^2 \rangle}}. \tag{7}$$

A value of ρ close to one indicates a perfect correspondence for the two patterns while a value close to zero indicates that the patterns are uncorrelated. In the course of the simulations, however, one oftentimes observes that the patterns are very alike but the cross-correlation is very small. Therefore, a more refined indicator is needed, which, though being less stringent than ρ, is related to a global spatial coincidence of the pattern with respect to the target pattern. The hexagonal target pattern has six marked modes located in the Fourier space; these modes show a unique wavelength and form a $\pi/3$ angle between each other in the Fourier plane. The new indicator compares the energy contained in the Fourier modes of the target pattern (e_t) with the energy contained in the actual pattern (e) at the same location in the Fourier plane:

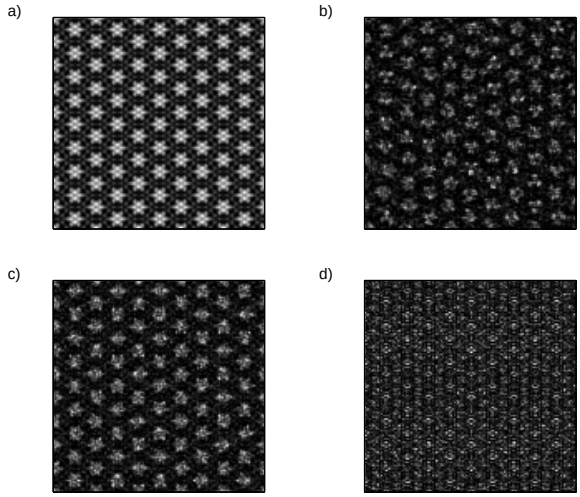

FIGURE 3. Influence of parameters c and np in the control. a) Hexagonal target pattern. b) Output pattern at $c = 0.6$ and $np = 4$. c) Controlled pattern at $c = 1$ and $np = 2$. d) Overshoot pattern for $c = 1.9$ and $np = 1$

$$S = e/e_t \tag{8}$$

In this way, $S = 1$ implies that the energy of the current pattern is located in the Fourier plane exactly in the same six points of the target pattern. This does not imply necessarily that $\rho = 1$ because the pattern can be distorted even when its spectral energy corresponds to the one of the target pattern.

In all the results presented in the following, Equation (1) is integrated from $t = 0$ until $t = 1,000$ with $\alpha I_0 = 1.7$. To eliminate transient effects, the evaluation of the indicators (ρ and S) is started at $t > 750$ and taken every $t = 1$. To reduce the fluctuations, the final values of ρ and S are the time average over the last 250 frames.

3. **Results.** Figure 3a shows the hexagonal target pattern. This pattern has been calculated from Equation (1) and stabilized with a Fourier filter. If not stabilized, this hexagonal pattern would be unstable for $\alpha I_0 = 1.7$. The two parameters of our analysis are c (the coupling strength) and np (the density of pinning points). Figure 3b shows a snapshot of the system where only imperfect stabilization is reached for $c = 0.6$ and $np = 4$ (the numerical values of the indicators are $\rho = 0.61$ and $S = 0.95$). In this case the pattern possesses the same orientation and only slightly different wave number ($k_b = 31.6\text{mm}^{-1}$) as compared to the target pattern ($k_a = 32.1\text{mm}^{-1}$), but the shape of the spots is heavily distorted.

By increasing the coupling strength c and the number of pinning points, the control of the target pattern improves. Eventually, for $c = 1$ and $np = 2$, the numerical values of the indicators are $\rho = 0.8$ and $S = 0.99$. This situation corresponds to Fig. 3c and in this case the actual pattern ($k_c = 32.2\text{mm}^{-1}$) is almost identical to the target one. If one increases the coupling strength further, one gets an overshoot

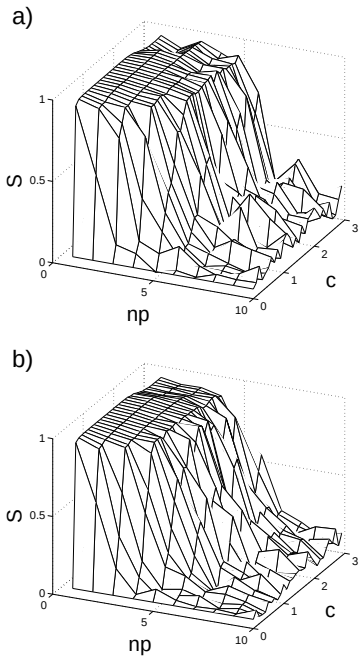

FIGURE 4. Influence of c and np on the indicator S: a) is for regular location pinning points, and b) is for randomly distributed pinning points.

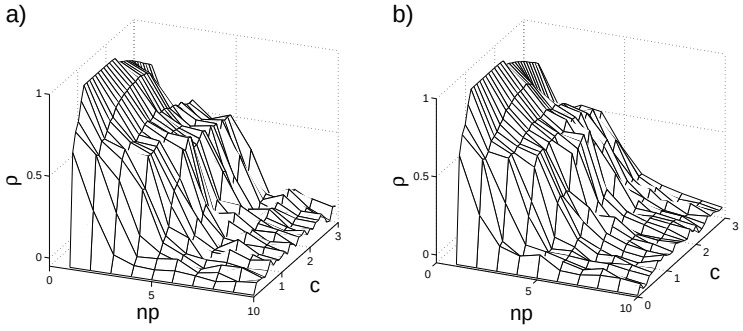

FIGURE 5. Influence of c and np on the correlation ρ: a) is for the regular location pinning points, and b) is for randomly distributed pinning points

pattern, as illustrated in Figure 3d, where the parameters are set to $c = 1.9$ and $np = 1$.

Let us now proceed to the exhaustive exploration of the control parameter space. This is done by taking $0 \leq c \leq 3$ and $1 \leq np \leq 10$ according to the Table I. The values of S are displayed in Figure 4, where panel (a) refers to the regular grid spacing and panel (b) refers to the random positioning of the pinning points. As expected, a reduction in the number of pinning points deteriorates the control

process. This reduction is slightly more pronounced in the random case than in the regular case.

The variation along parameter c indicates that the control process reaches an optimal effectiveness in the vicinity of $c = 1.5$. If $c > 2$, one observes a phenomenon of overshoot: the corrective term is exceedingly large and the control is consequently deteriorated. The same kind of behavior is observed for the other indicator ρ, which is displayed in Figure 5. Obviously, because this indicator is more stringent than S, only values of c close to optimum and $np = 1$ lead to $\rho \approx 1$. The results presented here for the stabilization of the LCLV are very reminiscent to the results obtained for the control and synchronization of the complex Ginzburg-Landau equation [10, 11]. In particular, we found that the efficiency of the control is proportional to the product of the density of pinning points by the coupling strength. We called this phenomenon *integral behavior* of the control [10].

4. **Discussion.** We have examined through numerical simulations the possibility of driving the actual pattern of an optical system to a target pattern which is an unstable solution of the system. In particular, we have shown that both the coupling strength and the density of pinning points are important to get a robust stabilization of the target pattern. It has been emphasized that the exact locations of the pinning points are not relevant. The advantage gathered by positioning the pinning points in a regular fashion is minute with respect to randomly distributed pinning points. This does not exclude the possibility that an optimal positioning function exists (which is neither random nor regular) able to further enhance the control process, leaving this space for further investigations in this direction.

Acknowledgments. Work partly supported by a MEC project (Spain) n. FIS2005-06912-C02-02 (DINCARD), Dr. C. Mendoza acknowledges financial support through PBCT project PSD-06. S.B. acknowledges the Yeshaya Horowitz Association through the Center for Complexity Science.

REFERENCES

[1] J. Garcia-Ojalvo and R. Roy, Phys. Rev. Lett. **86**, 5207, (2001).
[2] R. Ramaswani and K. Sivarajan, "Optical Networks:A Practical Perspective," Morgan Kaufman Publishers, 1998.
[3] P. Colet and R. Roy, Opt. Lett. **19**, 2056, (1994).
[4] J.P. Goedgebuer, L. Larger, and H. Porte, Phys. Rev. Lett. **80**, 2249, (1998).
[5] J.K. White and J.V. Moloney, Phys. Rev. A **59**, 2422, (1999).
[6] L. Pastur, L. Gostiaux, U. Bortolozzo, S. Boccaletti and P.L. Ramazza, Phys. Rev. Lett. **93**, 063902 (2004).
[7] S. Boccaletti, C. Grebogi, Y.-C. Lai, H. Mancini and D. Maza, Physics Report **329**, 103 (2000).
[8] S. Boccaletti, J. Kurths, G. Osipov, D.L. Valladares and C. Zhou, Physics Reports **366**, 1 (2002).
[9] L. Junge and U. Parlitz, Phys. Rev. **E61**, 3736 (2000).
[10] J. Bragard and S. Boccaletti, Phys. Rev. **E62**, 6346 (2000).
[11] S. Boccaletti and J. Bragard, Phil. Trans. Royal Soc. A, **364**, 2383 (2006).
[12] I. Aranson and L. Kramer, Rev. Mod. Phys., **74**, 99 (2002).
[13] F.T. Arecchi, S. Boccaletti and P.L. Ramazza, Phys. Reports **318**, 1 (1999).
[14] G.L. Oppo, G. D'Alessandro and W.J. Firth, Phys. Rev. **A44**, 471 (1991).
[15] P.L. Ramazza, S. Boccaletti, A. Giaquinta, E. Pampaloni, S. Soria and F.T. Arecchi, Phys. Rev. **A54**, 3472 (1996).
[16] P.L. Ramazza, S. Boccaletti and F.T. Arecchi, Opt. Comm. **136**, 267 (1997).

[17] M. Born and E. Wolf,"Principles of Optics: Electromagnetic Theory of Propagation, Interference and Diffraction of Light," Cambridge University Press (7th), 1999.
[18] A. De Wit, Advances Chem. Phys. **109** , 435 (1999).
[19] M.C. Cross and P.C. Hohenberg, Rev. Mod. Phys. **65** , 851 (1993).
[20] W.H. Press et al., "Numerical Recipe in C: the art of Scientific Computing," Cambridge University Press (2nd), 1992.

Received on November 15, 2006. Accepted on April 2, 2007.

E-mail address: cmendoza@ucv.cl